Cationic Substitutions in the "2201–1201" Intergrowth $HgTl_2Ba_4Cu_2O_{10}$

F. Goutenoire, M. Hervieu,* C. Martin, A. Maignan, C. Michel, F. Letouzé, and B. Raveau

Laboratoire CRISMAT, ISMRA / Université de Caen, CNRS URA 1318, Bd du Maréchal Juin, 14050 CAEN Cédex, France

Received February 23, 1994. Revised Manuscript Received June 15, 1994®

The study of the substitution of strontium for barium and of mercury for thallium in the cuprate $HgTl_2Ba_4Cu_2O_{10}$ has allowed two solid solutions to be synthesized, $HgTl_2Ba_{4-x}Sr_xCu_2O_{10}$ with $0 \le x \le 1.5$ and $Hg_{1+y}Tl_{2-y}Ba_4Cu_2O_{10+\delta}$ with $0 \le y \le 0.4$. The XRD and HREM studies of these phases confirm that they consist of regular intergrowths of the 1201 ($HgBa_2CuO_4$ type) with the 2201 ($Tl_2Ba_2CuO_6$ type) structures and show that barium and strontium are statistically distributed over the two kinds of $[AO]_\infty$ layers (A = Ba, Sr). The investigation of the superconducting properties shows that the as-synthesized phases are overdoped and do not superconduct but can be optimized by annealing in an hydrogenated argon flow. The substitution of thallium by mercury does not modify the superconducting properties; a T_c of 50 K is reached for $Hg_{1.4}Tl_{1.6}Ba_4Cu_2O_{10-\delta}$, i.e., close to that observed for $HgTl_2Ba_4Cu_2O_{10}$. On the opposite the substitution of strontium for barium leads to a rapid decrease of T_c for $HgTl_2Ba_{4-x}Sr_xCu_2O_{10}$, from 50 K for $x = 0$ to 30 K for $x = 0.8$, and superconductivity vanishes for $x > 0.8$.

Introduction

An important issue that concerns mercury based cuprates deals with the role of barium for the stabilization of these materials. The high-T_c superconductors $HgBa_2Ca_{m-1}Cu_mO_{3m+1}$ were indeed synthesized,[1-3] whereas the corresponding strontium cuprates could not be obtained even under high pressure, and a partial substitution of mercury by various cations was necessary to stabilize "Hg–Sr" cuprates.[4-11] Tl(III), owing to its $5d^{10}$ external configuration similar to that of Hg(II) and to its ability to form thallium mono- and bilayers, in barium as well as in strontium layered cuprates (see for review ref 12), is an interesting element for Hg(II) substitutions in these compounds. The recent synthesis of the 50 K superconductor $HgTl_2Ba_4Cu_2O_{10}$[13] has indeed shown the possibility of $[TlO]_\infty$ layers to coexist with $[HgO_\delta]_\infty$ layers in the same structure. This structure (Figure 1) can be described as an intergrowth of the "2201"-structure $Tl_2Ba_2CuO_6$ involving thallium bilayers, with the 1201 structure $HgBa_2CuO_4$, characterized by mercury monolayers. In the present paper, the substitution of strontium for barium in the latter cuprate, leading to the solid solution $HgTl_2Ba_{4-x}Sr_xCu_2O_{10-\delta}$, is investigated. Moreover the possible replacement of thallium by mercury in the thallium bilayers, leading to the homogeneity range $Hg_{1+y}Tl_{2-y}Ba_4Cu_2O_{10}$ is considered. The superconducting properties of these materials are reported.

Experimental Section

The compounds were prepared by the solid-state reaction of the oxides Tl_2O_3, HgO, BaO_2, SrO_2, and CuO. The oxides were intimately mixed in agate mortar, pressed in the form of pellets, and placed in alumina crucibles. They were heated in evacuated silica ampules in order to avoid volatilization of thallium and mercury.

Different thermal treatments were applied to the samples, varying the temperature, heating time, and the cooling rate. In the case of the oxide $HgTl_2Ba_{4-x}Sr_xCu_2O_{10}$, the best results were obtained by heating directly the mixtures of oxides at 850 °C for 10 h and then quenching to room temperature. These conditions differ from those used to synthesize the pure barium phase ($x = 0$) for which the cooling rate does not modify the purity of the phase.

The synthesis of the oxide $Hg_{1+y}Tl_{2-y}Ba_4Cu_2O_{10-\delta}$ was similar to that used for the pure barium oxide,[13] i.e., the mixture was heated progressively in 10 h at 800 °C, heated for 10 hours at this temperature and then slowly cooled to 400 °C in 10 h. The X-ray diffraction patterns were registered by step scanning over an angular range 2θ, with $3° \le 2\theta \le 80°$ in increment of 0.02° (2θ) on a Seifert diffractometer equipped with a primary monochromator in order to select the Cu $K\alpha_1$ radiation. The preset time was 6 s. The cell parameters and structure were refined by the Rietveld method with the

® Abstract published in *Advance ACS Abstracts,* August 15, 1994.

(1) Putilin, S. N.; Antipov, E. V.; Chmaissen, O.; Marezio, M. *Nature* **1993**, *362*, 226.
(2) Putilin, S. N.; Antipov, E. V.; Marezio, M. *Physica C* **1993**, *212*, 226.
(3) Schilling, A.; Cantoni, M.; Guo, J. D.; Ott, H. R. *Nature* **1993**, *363*, 56.
(4) Liu, R. S.; Hu, S. F.; Jefferson, D. A.; Edwards, P. P.; Hunneyball, P. D. *Physica C* **1993**, *205*, 206.
(5) Hu, S. F.; Jefferson, D. A.; Liu, R. S.; Edwards, P. P. *Solid State Chem.* **1993**, *103*, 280.
(6) Goutenoire, F.; Daniel, P.; Hervieu, M.; Van Tendeloo, G.; Michel, C.; Maignan, A.; Raveau, B. *Physica C* **1993**, *216*, 243.
(7) Pelloquin, D.; Michel, C.; Van Tendeloo, G.; Maignan, A.; Hervieu, M.; Raveau, B. *Physica C* **1993**, *214*, 87.
(8) Pelloquin, D.; Hervieu, M.; Michel, C.; Van Tendeloo, G.; Maignan, A.; Raveau, B. *Physica C* **1993**, *216*, 257.
(9) Hervieu, M.; Van Tendeloo, G.; Maignan, A.; Michel, C.; Goutenoire, F.; Raveau, B. *Physica C* **1993**, *216*, 264.
(10) Maignan, A.; Van Tendeloo, G.; Hervieu, M.; Michel, C.; Raveau, B. *Physica C* **1993**, *212*, 239.
(11) Maignan, A.; Michel, C.; Van Tendeloo, G.; Hervieu, M.; Raveau, B. *Physica C* **1993**, *216*, 1.
(12) *Thallium-based high temperature superconductors*; Hermann, A. M.; Yakhmi, J. V., Eds.; Marcel Dekker: New York, 1993.
(13) Martin, C.; Huvé, M.; Van Tendeloo, G.; Maignan, A.; Michel, C.; Hervieu, M.; Raveau, B. *Physica C* **1993**, *212*, 274.

0897-4756/94/2806-1654$04.50/0

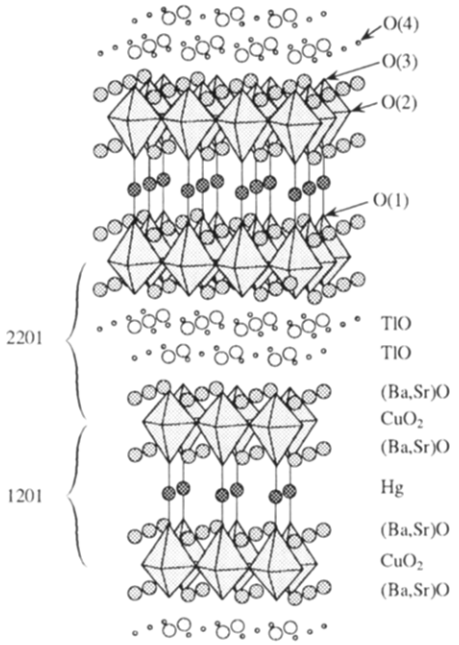

Figure 1. Idealized structure of the $HgTl_2Ba_4Cu_2O_{10}$ built up from the intergrowth of "2201" and 1201 structural units.

computer program DBW 3.2.[14] The electron diffraction study was carried out with a JEOL 200 CX electron microscope fitted with a side-entry goniometer. The high-resolution electron microscopy (HREM) was performed with a TOPCON 002B microscope having a point resolution of 1.8 Å. The energy-dispersive X-ray microanalysis (EDS) was performed with a Kevex analyser.

Magnetic measurements were performed with a SQUID magnetometer in the temperature range 4.2−60 K. The samples were first zero field cooled to 4.2 K, and then a magnetic field of 10^{-3} T was applied. The magnetization versus temperature curve was registered from 4.2 K to $T > T_c$. Samples were tested in the form of powders in order to eliminate grain boundary effects, i.e., the magnetization measurements are more sensitive to intragranular superconductivity. No demagnetization corrections were performed.

Results and Discussion

For the above experimental conditions, a single phase $HgTl_2Ba_{4-x}Sr_xCu_2O_{10}$ is obtained for $0 \le x \le 1.5$. The electron diffraction investigation and reconstruction of the reciprocal space evidence a tetragonal cell with $a \sim a_p \sim 3.85$ Å and $c \sim 42$ Å $= c_{2201} + 2c_{1201}$; the conditions limiting the reflection are $h + k + l = 2n$, as shown from Figure 2. The cell parameters, refined from XRD patterns (Figure 3), decrease continuously (Table 1, Figure 4) as x increases in agreement with the smaller size of Sr^{2+} compared to Ba^{2+}. For $x = 1.7$ which corresponds to a multiphasic sample, the refined lattice parameters are very close to those obtained for $x = 1.5$ and confirm the limit of the solid solution.

The study of the substitution of mercury for thallium shows, for the phase $Hg_{1+y}Tl_{2-y}Ba_4Cu_2O_{10-\delta}$, a smaller homogeneity range: $0 \le y \le 0.4$. Note that the limit $y = 0.4$, confirmed the EDS analysis, corresponds exactly to the maximum mercury content that could be introduced in the 2223 thallium cuprate,[15] leading to the formulation $Tl_{1.6}Hg_{0.4}Ba_2Ca_2Cu_3O_{10-\delta}$. This suggests

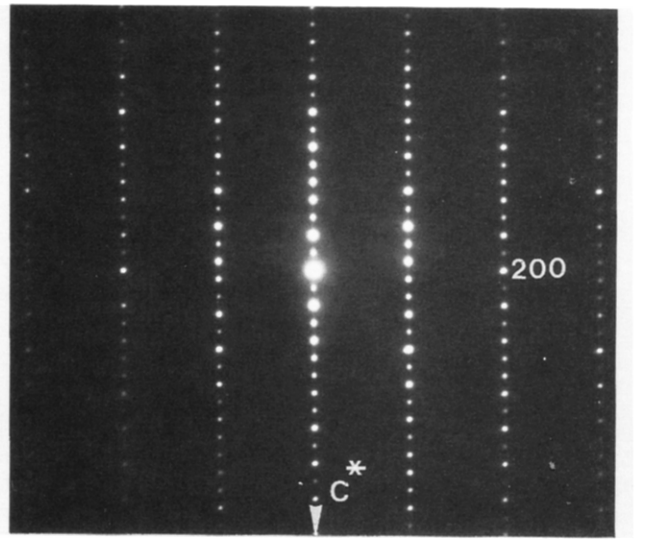

Figure 2. [010] electron diffraction pattern.

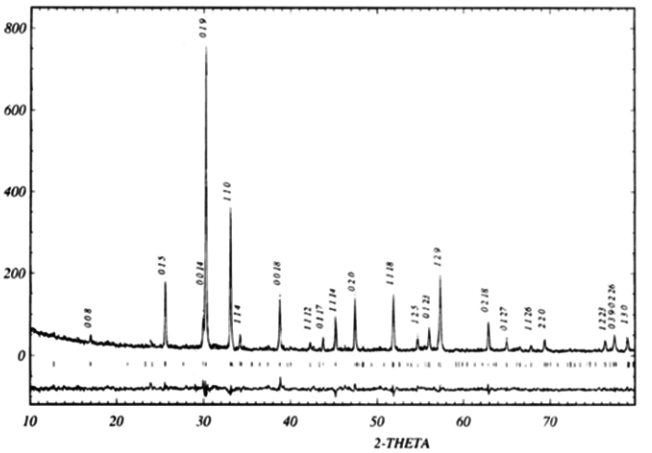

Figure 3. Experimental (dotted line), and calculated and difference (solid lines) XRD patterns for $HgTl_2Ba_4Cu_2O_{10}$. Marks correspond to Bragg angle positions. Some of the main diffraction peaks are indexed.

Table 1. Refined Cell Parameters

composition	a (Å)	c (Å)
	$HgTl_2Ba_{4-x}Sr_xCu_2O_{10}$	
$x = 0$	3.8567(7)	42.158(1)
$x = 0.2$	3.8518(1)	42.123(2)
$x = 0.6$	3.8396(2)	41.918(2)
$x = 0.8$	3.8345(1)	41.823(1)
$x = 1$	3.8289(1)	41.757(1)
$x = 1.2$	3.8224(2)	41.668(4)
$x = 1.5$	3.8160(2)	41.536(4)
$x = 1.7$	3.8164(3)	41.533(5)
	$Hg_{1+y}Tl_{2-y}Ba_4Cu_2O_{10-\delta}$	
$y = 0.4$	$a = 3.851(5)$	$c = 42.16(3)$

that in the present case mercury is not distributed statistically between two sorts of layers but that the "1201" layers contain only mercury, whereas the additional mercury is substituted for thallium at random in the 2201 structure, according to the formula $[HgBa_2CuO_4]^{1201}[Tl_{2-y}Hg_yBa_2CuO_6]^{2201}$. The electron diffraction study confirms that the symmetry does not vary in all the homogeneity range. The comparison of the cell parameters of $HgTl_2Ba_{4-x}Sr_xCu_2O_{10}$ ($y = 0$) and of the limit composition $Hg_{1.4}Tl_{1.6}Ba_4Cu_2O_{10-\delta}$ ($y = 0.4$, Table

(14) Wiles, D. B.; Young, R. A. *J. Appl. Crystallogr.* **1981**, *14*, 149.
(15) Goutenoire, F.; Maignan, A.; Van Tendeloo, G.; Martin, C.; Michel, C.; Hervieu, M.; Raveau, B. *Solid State Commun.* **1994**, *90*, 47.

(16) Martin, C.; Maignan, A.; Huvé, M.; Michel, C.; Hervieu, M.; Raveau, B. *Eur. J. Solid State Inorg. Chem.* **1993**, *30*, 7.

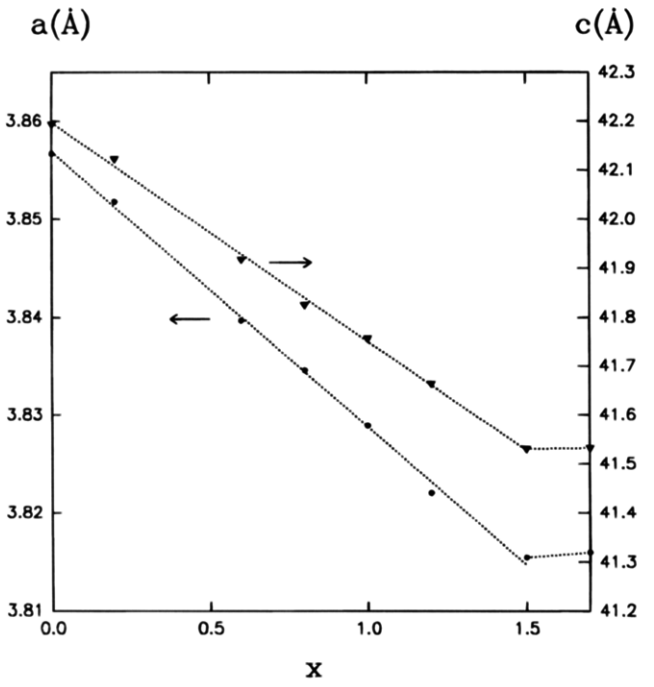

Figure 4. Evolution of a and c parameters versus x in the solid solution $HgTl_2Ba_{4-x}Sr_xCu_2O_{10}$.

1) shows that these parameters do not vary significantly as thallium is replaced by mercury. This feature is consistent with the results observed in the Tl/Hg "2223"[15] and "1212"[17] cuprates.

The HREM investigation, selecting the [100] images, allowed the layer stacking mode to be checked. They are identical whatever the composition x or y may be. One of the characteristic images is shown for $HgTl_2Ba_{2.5}Sr_{1.5}Cu_2O_{10}$ on Figure 5. The cationic positions are imaged as black dots: groups of three and four staggered rows of black dots alternate, separated by single rows of smaller dots. They are correlated to two groups of layers, [AO]–[HgO]–[AO] and [AO]–[TlO]–[TlO]–[AO], respectively, that are separated by single $[CuO_2]$ layers (A = Ba, Sr). Such an interpretation is in agreement with the comparison of the theoretical images calculated, for a focus value close to −200 Å, from the refined positions and confirms that the structure of these oxides is built up from the intergrowth of 2201 and 1201 structural units (Figure 1). Note that no sign of Ba/Sr ordering can be detected from the HREM images, an even contrast being systematically observed.

In a general way, the stacking of the layers along $\vec{c}$ is highly regular; it is only sometimes broken by the formation of intergrowth defects. An example is shown in Figure 6. For a focus value close to 0 nm, the $[CuO_2]_\infty$ layers are highlighted and the mercury is indicated by white arrowheads; in the middle of the image (curved black arrow), an additional 1201 unit is intercaled in the matrix, involving the existence of two adjacent 1201's, i.e., of the local formation of a $[HgBa_2CuO_4]^{1201}{}_2$ $[Tl_{2-y}Hg_yBa_2CuO_6]^{2201}$ member of the family.

Taking into account the good cristallinity of the sample and the regularity of the layer stacking, structural calculations were performed on the sample $x = 1$, $HgTl_2Ba_3SrCu_2O_{10}$; they were carried out in the space group *I4/mmm* for the 92 *hkl*, included in the angular

(17) Letouzé, F.; Peluau, S.; Michel, C.; Maignan, A.; Martin, C.; Hervieu, M.; Raveau, B. *J. Mater. Chem.*, submitted.

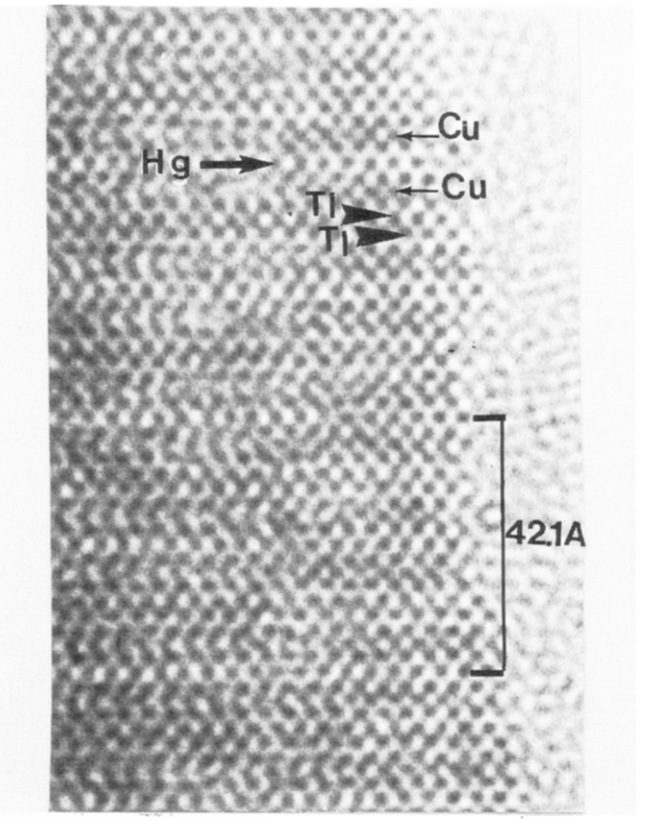

Figure 5. [100] HREM image of the sample. Hg, Tl, and Cu atom positions are indicated.

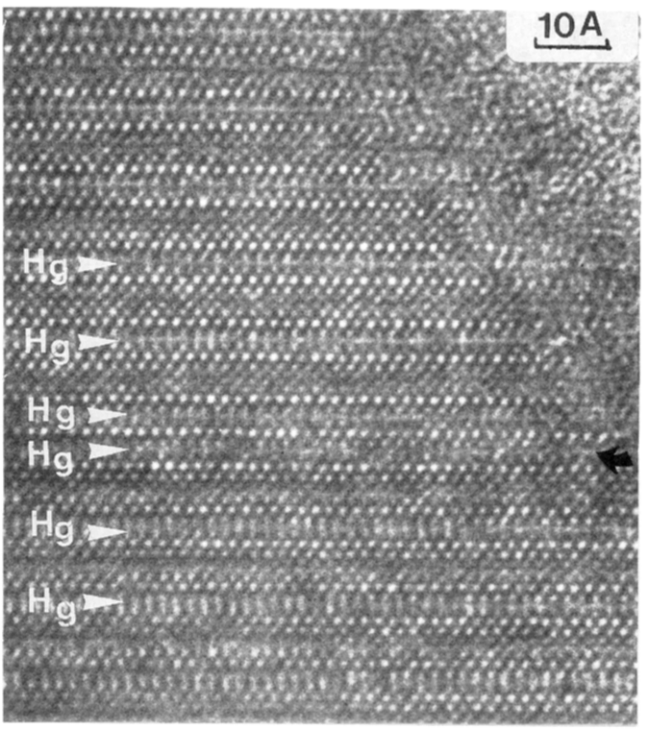

Figure 6. Example of intergrowth defect corresponding to the existence of two adjacent "1201" units. The [HgO] layers are indicated by white arrow heads.

interval $10° \leq 2\theta \leq 80°$. The positions of the cations and of the oxygen atoms, and finally the thermal factors of the heavy atoms were refined successively. The B factors of the oxygen atoms were arbitrarily fixed at 1 Å^2. The refinement of the occupancy factors of the metallic sites confirmed the nominal cationic composition. In these conditions the R_I factor was lowered to

Table 2. Crystallographic Parameters of $HgTl_2Ba_3SrCu_2O_{10}$ *I4/mmm*, a = 3.8289(1) and 41.757(1) Å

atom	site	x	y	z	B (Å^2)[a]
Hg	2a	0.0	0.0	0.0	1.8(3)
Tl	4e	0.0	0.0	0.2237(1)	0.7(1)
Cu	4e	0.0	0.0	0.1135(4)	0.0(3)
(Ba, Sr)$_1$	4e	0.5	0.5	0.0664(2)	1.7(3)
(Ba, Sr)$_2$	4e	0.5	0.5	0.1596(2)	1.0(4)
O_1	4e	0.0	0.0	0.050(1)	1.0[b]
O_2	8g	0.5	0.0	0.114(1)	1.0[b]
O_3	4e	0.0	0.0	0.174(2)	1.0[b]
O_4	4e	0.5	0.5	0.228(2)	1.0[b]

[a] R_p = 10.2%, R_{wp} = 13.2%; R_i = 7.5%. [b] B factors for oxygen are arbitrarily fixed.

Table 3. Interatomic Distances for $HgTl_2Ba_3SrCu_2O_{10}$ (a) and Compared with Those Calculated for $HgTl_2Ba_4Cu_2O_{10}$ (b)

	(a)	(b)
Hg–O_1	2.09(6) × 2	2.10(5) × 2
Tl–O_3	2.06(7) × 1	1.84(4) × 1
Tl–O_4	2.71(4) × 4	2.737(4) × 4
Tl–O_4	1.99(6) × 1	1.98(5) × 1
Cu–O_1	2.66(6) × 1	2.68(6) × 1
Cu–O_2	1.915(1) × 4	1.929(1) × 4
Cu–O_3	2.52(7) × 1	2.82(5) × 1
(Ba, Sr)$_1$–O_1	2.79(1) × 4	2.83(1) × 4
(Ba, Sr)$_1$–O_2	2.76(3) × 4	2.76(2) × 4
(Ba, Sr)$_2$–O_2	2.70(3) × 4	2.73(2) × 4
(Ba, Sr)$_2$–O_3	2.74(2) × 4	2.86(1) × 4
(Ba, Sr)$_2$–O_4	2.90(6) × 1	2.93(5) × 1

0.075 for the atomic coordinates listed in Table 2. Although the positions of the oxygen atoms were not determined with accuracy, the interatomic distances (Table 3) allow several features to be emphasized:

(i) The refinement of the occupancy of the two kinds of A sites (Ba, Sr) shows that no ordering phenomenon occurs between barium and strontium in agreement with the HREM observations. The very similar A–O distances observed for the two kinds of A sites are also in agreement with such an aleatory distribution of barium and strontium in the AO layers.

(ii) No difference is observed on the Tl and Hg sites. It is of course not possible to determine any ordering between these two elements owing to their similar atomic numbers. Nevertheless from structural considerations, it appears clearly that mercury should occupy preferentially the "1201" layers rather than the "2201" layers owing to its ability to take the dumbbell coordiation. The quasi-absence of oxygen in the "1201" layer supports this view point. The introduction of one additional oxygen in this layer increases the R_I factor up to 0.085. This shows that this layer is probably highly oxygen deficient, in agreement with neutron diffraction studies of $HgBa_2Ca_{m-1}Cu_mO_{3m+1}$ superconductors.[1,2] Moreover the HREM images show that, at this level, the contrast is different from that observed for the $[TlO]_\infty$ layers, for several focus values; this is confirmed by image calculations. Owing to the scattering factors of Hg and Tl, which are very close, such a phenomenon is supposed to originate in the environment of the cation, i.e., the absence of oxygen. Thus these results support the cationic distribution represented by the formula $(HgBa_2CuO_4)(Tl_{1.6}Hg_{0.4}Ba_2CuO_{6-\delta})$ for the mercury-rich phase.

(iii) One observes a rather large decrease of the Cu–O apical distances of the CuO_6 octahedra compared to the pure barium phase (Table 3). Nevertheless the lack of accuracy on the oxygen positions does not allow any conclusion to be drawn in the absence of neutron diffraction data.

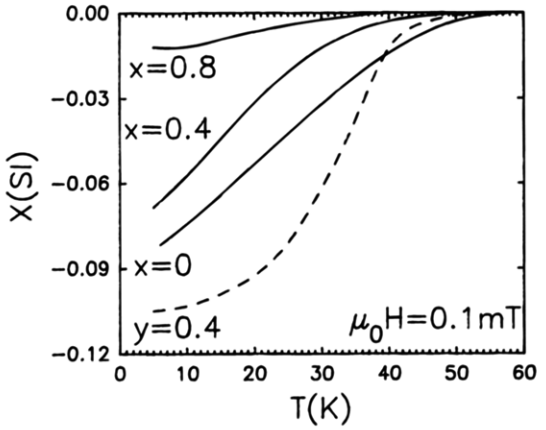

Figure 7. Temperature dependence of the magnetic susceptibility $\chi(T)$ for $HgTl_2Ba_{4-x}Sr_xCu_2O_{10}$ and $Hg_{1+y}Tl_{2-y}Ba_4Cu_2O_{10-\delta}$ samples after optimization in a reducing flow (Ar/H_2 90/10%, T = 220 °C); the curves correspond to $x = 0$, $x = 0.4$, $x = 0.8$, and $y = 0.4$.

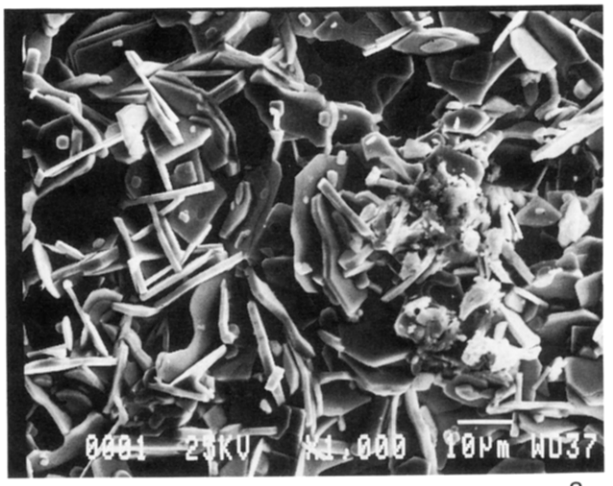

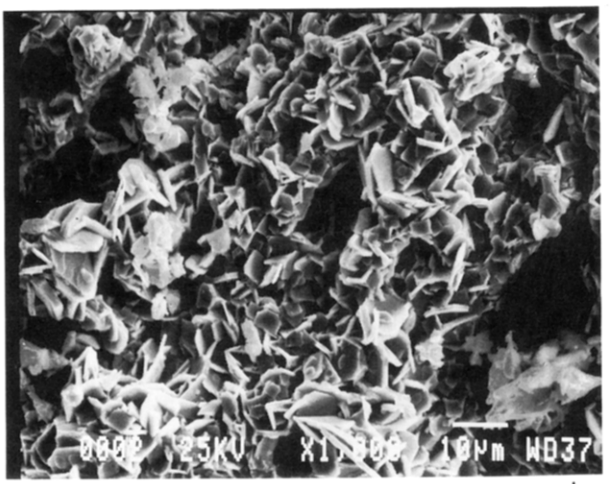

Figure 8. SEM images of $x = 0$ and $x = 0.6$ samples showing the evolution of the grain size with the strontium content.

Similar to the phase of $HgTl_2Ba_4Cu_2O_{10}$, the as-synthesized oxides $HgTl_2Ba_{4-x}Sr_xCu_2O_{10}$ and $Hg_{1+y}Tl_{2-y}Ba_4Cu_2O_{10-\delta}$ do not superconduct. In the same way, superconductivity can be induced by annealing the

samples in an hydrogenated argon flow (10% H_2) at 220 °C, showing that the as-synthesized compounds are overdoped. One indeed observes (Figure 7) that the mercury-rich phase $Hg_{1.4}Tl_{1.6}Ba_4Cu_2O_{10}$ exhibits a critical temperature of 50 K after annealing, with a diamagnetic volume fraction of 10%. In the same way superconductivity can be induced in the oxide $HgTl_2Ba_{4-x}Sr_xCu_2O_{10}$ for $0 \leq x \leq 0.8$. Nevertheless, the T_c's decrease from 50 K for $x = 0$ to 30 K for $x = 0.8$ (Figure 7), and all attempts to generate superconductivity for $x > 0.8$ were unsuccessful. This rapid decrease of superconductivity as barium is replaced by strontium was also observed for the "2201" cuprate $Tl_2Ba_{2-x}Sr_xCuO_6$.[16] In all cases, one observes a broad character of the transition. An important feature deals with the rapid decrease of the superconductivity volume fraction when strontium is introduced into the matrix, from 8% for $x = 0$ to 1% for $x = 0.8$. In fact one must take into consideration the microstructure of these samples (Figure 8). One indeed observes that the size of the grains about 20 μm or less for $x = 0$ (Figure 8a), is much smaller for $x = 0.6$, i.e., generally less than 5 μm (Figure 8b). This decrease of the grain size is not favorable to superconductivity, since if one takes into consideration the penetration depth in thallium-based superconductors $\lambda_{ab} \sim 0.2$ μm, this would produce small superconducting volume fractions.

Concluding Remarks

This study confirms the difficulty to stabilize mercury based cuprates with pure $[SrO]_\infty$ layers and shows the negative effect of strontium on the superconducting properties of these materials. On the opposite, the partial replacement of thallium by mercury does not influence the superconducting properties of these oxides in agreement with the previous results on the "2223" cuprate $Tl_{2-x}Hg_xBa_2Ca_2Cu_3O_{10}$.[15] Investigations of these systems under high pressure should be performed to understand the behavior of thallium in the presence of mercury, as well as that of strontium in the presence of mercury.